

A New 700 GeV Scalar in the LHC Data?

Maurizio Consoli¹ and George Rupp²

¹INFN, Sezione di Catania, 95123 Catania, Italy

²CeFEMA and CFTP, Instituto Superior Técnico, Universidade de Lisboa, 1049-001 Lisboa, Portugal

Abstract

As an alternative to the metastability of the electroweak vacuum, resulting from perturbative calculations, one can consider a nonperturbative effective potential which, as at the beginning of the Standard Model, is restricted to the pure Φ^4 sector yet consistent with the known analytical and numerical studies. In this approach, where the electroweak vacuum is now the lowest-energy state, besides the resonance of mass $m_h = 125$ GeV defined by the quadratic shape of the potential at its minimum, the Higgs field should exhibit a second resonance with mass $(M_H)^{\text{Theor}} = 690$ (30) GeV associated with the zero-point energy determining the potential depth. In spite of its large mass, this resonance would couple to longitudinal W s with the same typical strength as the low-mass state at 125 GeV and represent a relatively narrow resonance, mainly produced at LHC by gluon-gluon fusion. In this paper, we review LHC data suggesting a new resonance of mass $(M_H)^{\text{EXP}} \sim 682$ (10) GeV, with a statistical significance that is far from negligible.

Keywords: Higgs mass spectrum, LHC experiments

DOI: 10.31526/LHEP.2024.515

1. INTRODUCTION

The discovery [1, 2] of a narrow scalar resonance with mass $m_h = 125$ GeV and the phenomenological consistency with the expectations for the Higgs boson have confirmed spontaneous symmetry breaking (SSB) through the Higgs field as a fundamental ingredient of current particle physics. Yet, in our opinion, the present perturbative description of symmetry breaking is not entirely satisfactory. Indeed, if we look beyond the Fermi scale, such a calculation predicts that the effective potential of the Standard Model (SM) should have a new minimum, far beyond the Planck scale and much deeper than the electroweak (EW) vacuum; see, e.g., [3, 4]. While it is reassuring that the most accurate calculation [5] gives a tunneling time that is larger than the age of the universe, still the idea of a metastable vacuum raises several questions: the role of gravitational effects and the mechanism explaining why the theory remains trapped in our EW vacuum. This would require a cosmological perspective and controlling the properties of matter in the extreme conditions of the early universe.

As an alternative, one can consider [6, 7, 8, 9] a nonperturbative effective potential which, as at the beginning of the SM, is restricted to the pure Φ^4 sector but is also consistent with the known analytical and numerical studies. In this approach, where the EW vacuum is now the lowest-energy state, besides the resonance of mass $m_h = 125$ GeV defined by the quadratic shape of the potential at its minimum, the Higgs field should exhibit a second resonance with a mass $(M_H)^{\text{Theor}} = 690$ (30) GeV, associated with the zero-point energy (ZPE) determining the potential depth. This large M_H stabilises the potential, because including the ZPEs of all known gauge and fermion fields would now represent just a small radiative correction.¹ Like in the early days of the SM, one could thus adopt the perspective of explaining SSB within the pure scalar sector.

¹By subtracting quadratic divergences or using dimensional regularisation, the logarithmically divergent terms in the ZPEs of the various fields are proportional to the fourth power of the mass. Thus, in units of the pure scalar term, one finds $(6M_w^4 + 3M_Z^4)/M_H^4 \lesssim 0.002$ and $12m_f^4/M_H^4 \lesssim 0.05$.

Checking this picture then requires observing the second resonance and its phenomenology.

In this respect, the hypothetical H is not like a regular Higgs boson of 700 GeV, because it would couple to longitudinal W s with the same typical strength as the low-mass state at 125 GeV [6, 7, 8, 9]. In fact, it is $m_h = 125$ GeV (and not $M_H \sim 700$ GeV) which fixes the quadratic shape of the potential and the interaction with the Goldstone bosons. Thus, the large conventional widths $\Gamma(H \rightarrow ZZ + WW) \sim G_F M_H^3$ would be suppressed by the small ratio $(m_h/M_H)^2 \sim 0.032$, leading to the estimates $\Gamma(H \rightarrow ZZ) \sim M_H/(700 \text{ GeV}) \times (1.6 \text{ GeV})$ and $\Gamma(H \rightarrow WW) \sim M_H/(700 \text{ GeV}) \times (3.3 \text{ GeV})$. As such, the heavy H should be a relatively narrow resonance of total width $\Gamma(H \rightarrow \text{all}) = 25 \div 35$ GeV, decaying predominantly to $t\bar{t}$ quark pairs, with a branching ratio of about 70 \div 80%. Due to its small coupling to longitudinal W s, H production through vector-boson fusion (VBF) would also be negligible as compared to gluon-gluon fusion (ggF), which has a typical cross section $\sigma^{\text{ggF}}(pp \rightarrow H) \sim 1100$ (170) fb [14, 15], depending on the QCD and H -mass uncertainties.

After this brief review, in this paper, we will present LHC data suggesting a new resonance in the expected mass and width range, with a nonnegligible statistical significance. Partial evidence was already presented in [10, 11, 12, 13], but in Section 2, we will consider a larger data set and also refine the analysis of some final states. Finally, Section 3 will contain a summary and our conclusions.

2. EXPERIMENTAL SIGNALS FROM LHC

Having a definite prediction $(M_H)^{\text{Theor}} = 690$ (30) GeV, we will look for signals in the expected region of invariant mass 600 \div 800 GeV, so that local deviations from the background should not be downgraded by the “look elsewhere” effect. In this search, one should also keep in mind that, with the present energy and luminosity of LHC, the second resonance is too heavy to be seen unambiguously in all possible channels. (Recall the $h(125)$ discovery, which initially was producing no signals in the important $b\bar{b}$ and $\tau^+\tau^-$ channels.)

Now, with an expected large branching ratio $B(H \rightarrow t\bar{t}) = (70 \div 80)\%$, the natural starting point would be the $t\bar{t}$ channel.

However, in the relevant region $m(t\bar{t}) = 620 \div 820$ GeV, CMS measurements [16] give a background cross section $\sigma(pp \rightarrow t\bar{t}) = 107 \pm 7.6$ pb, which is about 100 times larger than the expected signal $\sigma(pp \rightarrow H \rightarrow t\bar{t}) \lesssim 1$ pb. Therefore, in [10, 11, 12, 13], the analysis was focused on available channels with a relatively smaller background, namely:

- (i) ATLAS ggF-like 4-lepton events,
- (ii) ATLAS high-mass inclusive $\gamma\gamma$ events,
- (iii) ATLAS and CMS ($b\bar{b} + \gamma\gamma$) events,
- (iv) CMS $\gamma\gamma$ pairs produced in pp diffractive scattering.

2.1. The ATLAS ggF-Like 4-Lepton Events

To start with, we will review ATLAS work [17, 18] dedicated to the charged 4-lepton channel and to the search for a heavy scalar resonance H decaying through the chain $H \rightarrow ZZ \rightarrow 4l$. This is important because, for this particular channel, there is a precise prediction characteristic of our picture. Indeed, for a relatively narrow resonance, the resonant peak cross section $\sigma_R(pp \rightarrow H \rightarrow 4l)$ can be well approximated as

$$\sigma_R(pp \rightarrow H \rightarrow 4l) \sim \sigma(pp \rightarrow H)B(H \rightarrow ZZ)4B^2(Z \rightarrow l^+l^-), \quad (1)$$

with $4B^2(Z \rightarrow l^+l^-) \sim 0.0045$. Thus, in our case, where $\Gamma(H \rightarrow ZZ) \sim M_H/(700 \text{ GeV}) \times (1.6 \text{ GeV})$ and $\sigma(pp \rightarrow H) \sim \sigma_{\text{ggF}}(pp \rightarrow H) \sim 1100$ (170) fb, by introducing the reduced width $\gamma_H = \Gamma(H \rightarrow \text{all})/M_H$, we find the sharp correlation

$$\gamma_H \times \sigma_R(pp \rightarrow H \rightarrow 4l)^{\text{Theor}} \sim (0.011 \pm 0.002) \text{ fb}, \quad (2)$$

to be compared with the ATLAS data.

In the ATLAS search, the 4-lepton events were divided into ggF-like and VBF-like events. By expecting our second resonance to be produced through gluon-gluon fusion, we have considered the ggF-like category. The only sample that satisfies the two requirements, namely, (a) being homogeneous from the point of view of the selection and (b) having sufficient statistics, is the so-called ggF-low category, which contains a mixture of all three final states. Since for an invariant mass around 700 GeV, the energy resolution of these events varies considerably,² it is natural to adopt a large-bin visualization to avoid spurious fluctuations between adjacent bins. The numbers of events are reported in Table 1 [17, 18].

Now, subtracting the background from the observed events gives a considerable excess, at about 680 GeV, and then a sizable defect, around 740 GeV. A simple explanation for these two simultaneous features would be the existence of a resonance of mass $M_H \sim 700$ GeV which, above the Breit-Wigner peak, produces the characteristic negative-interference pattern proportional to $(M_H^2 - s)$. To check this idea, we have exploited the basic model where the ZZ pairs, each subsequently decaying into a charged l^+l^- pair, are produced by various mechanisms at the parton level. For $E \equiv m(4l)$, this produces a smooth distribution of background events $N_b(E)$, proportional to a background cross section $\sigma_b(E)$, which can interfere with a resonance of mass M_H and total decay width Γ_H . The total cross

E [GeV]	$N_{\text{EXP}}(E)$	$N_{\text{B}}(E)$	$N_{\text{EXP}}(E) - N_{\text{B}}(E)$
560(30)	38 ± 6.16	32.0	6.00 ± 6.16
620(30)	25 ± 5.00	20.0	5.00 ± 5.00
680(30)	26 ± 5.10	13.04	12.96 ± 5.10
740(30)	3 ± 1.73	8.71	-5.71 ± 1.73
800(30)	7 ± 2.64	5.97	1.03 ± 2.64

TABLE 1: For luminosity 139 fb^{-1} , we give the ATLAS ggF-low events $N_{\text{EXP}}(E)$ and the estimated background $N_{\text{B}}(E)$ [17, 18] for invariant mass $m_{4l} = E = 530 \div 830$ GeV. To avoid spurious migrations between neighbouring bins, we group the data into bins of 60 GeV, corresponding to the 10 bins of 30 GeV from 545 (15) GeV to 815 (15) GeV; see [18].

section $\sigma_T(E)$ can then be expressed as [8]

$$\sigma_T(E) = \sigma_b(E) + \frac{2(M_H^2 - s)\Gamma_H M_H}{(s - M_H^2)^2 + (\Gamma_H M_H)^2} \sqrt{\sigma_R \sigma_b(E)} + \frac{(\Gamma_H M_H)^2}{(s - M_H^2)^2 + (\Gamma_H M_H)^2} \sigma_R, \quad (3)$$

where we have introduced the resonant peak cross section σ_R at $s = M_H^2$.

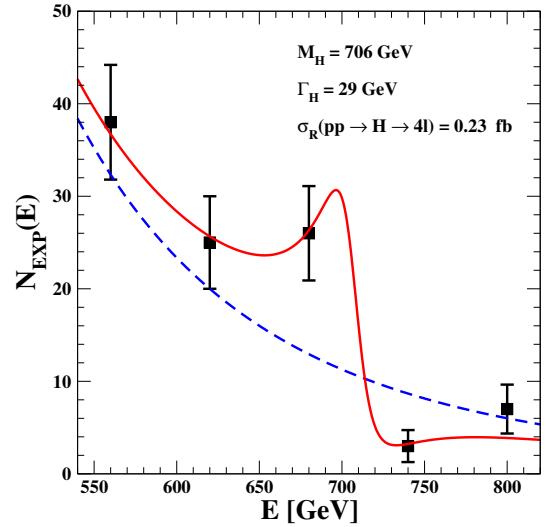


FIGURE 1: The values $N_{\text{EXP}}(E)$ in Table 1 vs. the corresponding $N_{\text{TH}}(E)$ in equation (4) (the full red curve). The resonance parameters are $M_H = 706$ GeV, $\gamma_H = 0.041$, $\sigma_R = 0.23$ fb, and the ATLAS background (dashed blue curve) is approximated as $N_b(E) = A \times (710 \text{ GeV}/E)^\nu$, with $A = 10.55$ and $\nu = 4.72$.

Then, by simple redefinitions, the theoretical number of events can be expressed as

$$N_{\text{TH}}(E) = N_b(E) + \frac{P^2 + 2Px(E)\sqrt{N_b(E)}}{\gamma_H^2 + x^2(E)}, \quad (4)$$

where $x(E) = (M_H^2 - E^2)/M_H^2$, $P \equiv \gamma_H \sqrt{N_R}$, and $N_R = \sigma_R \mathcal{A} 139 \text{ fb}^{-1}$ denotes the extra events at the resonance peak for an acceptance \mathcal{A} . The data in Table 1 were fitted with equation (4) in [12, 13]. The results are $M_H = 706$ (25) GeV, $P = 0.14 \pm 0.07$, and $\gamma_H = 0.041 \pm 0.029$, corresponding to a total

²The resolution varies from about 12 GeV for $4e$ events to 19 GeV for $2e2\mu$, up to 24 GeV for 4μ .

Bin [GeV]	σ_{EXP} [fb]	σ_{B} [fb]	$(\sigma_{\text{EXP}} - \sigma_{\text{B}})$ [fb]
555–585	0.252 ± 0.056	0.272 ± 0.023	-0.020 ± 0.060
585–620	0.344 ± 0.070	0.259 ± 0.021	$+0.085 \pm 0.075$
620–665	0.356 ± 0.075	0.254 ± 0.023	$+0.102 \pm 0.078$
665–720	0.350 ± 0.073	0.214 ± 0.019	$+0.136 \pm 0.075$
720–800	0.126 ± 0.047	0.206 ± 0.018	-0.080 ± 0.050
800–900	0.205 ± 0.052	0.152 ± 0.017	$+0.053 \pm 0.055$

TABLE 2: The observed ATLAS cross section [19, 20] and estimated background for a 4-lepton invariant mass $m(4l) \equiv E$ from 555 to 900 GeV. These values are obtained by multiplying the bin size with the average differential cross sections $\langle (d\sigma/dE) \rangle$, reported for each bin in the companion HEPData file [20]. The full background cross section σ_{B} contains a dominant contribution from $q\bar{q} \rightarrow 4l$ events.

width $\Gamma_H = 29 \pm 20$ GeV. One thus obtains $N_R \sim 12_{-9}^{+15}$ and for acceptance $\langle \mathcal{A} \rangle \sim 0.38$, by averaging the two extremes 0.30 and 0.46 for the ggF-like category of events [17], $\sigma_R \sim 0.23_{-0.17}^{+0.28}$ fb. A graphical comparison is shown in Figure 1.

The quality of the fit is good, but error bars are large and a test of our picture is not very stringent. Still, with our $\Gamma(H \rightarrow ZZ) \sim 1.6$ GeV, for $M_H \sim 700$ GeV, and the central fitted $\langle \Gamma_H \rangle = 29$ GeV, we find a branching ratio $B(H \rightarrow ZZ) \sim 0.055$ which, for the theoretical value $\sigma^{\text{ggF}}(pp \rightarrow H) \sim 923$ fb of [15] (at $M_H = 700$ GeV) would imply a theoretical peak cross section $(\sigma_R)^{\text{Theor}} = 923 \times 0.055 \times 0.0045 \sim 0.23$ fb, coinciding with the central value from our fit. Also, from the central values $\langle \sigma_R \rangle = 0.23$ fb and $\langle \gamma_H \rangle = 0.041$, we find $\langle \sigma_R \rangle \langle \gamma_H \rangle \sim 0.0093$ fb, consistent with equation (2).

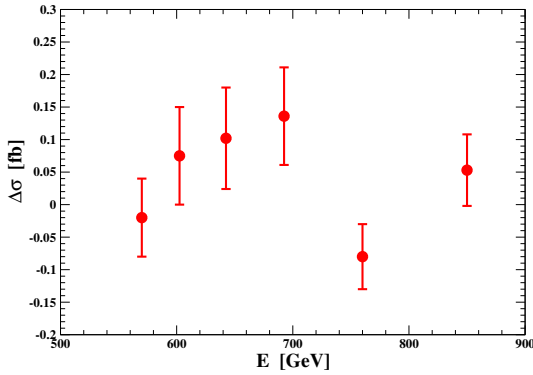


FIGURE 2: The quantity $\Delta\sigma = (\sigma_{\text{EXP}} - \sigma_{\text{B}})$ given for each bin in the last column of Table 2.

After this first comparison from [12, 13], we will now consider the other ATLAS paper [19, 20] for the differential 4-lepton cross section $d\sigma/dE$, with $E = m(4l)$. From Figure 5 of [19], one finds the same excess-defect sequence as in Table 1 and additional support for a new resonance. The corresponding data are given in Table 2 and Figure 2. Besides, by comparing with [19, 20], we can sharpen our analysis. In fact, the ggF-like events considered above contain a large contribution from $q\bar{q} \rightarrow 4l$ processes. Although the initial state is pp in all cases, our H resonance would mainly be produced through gluon-gluon fusion, so that, strictly speaking, the interference should only be computed with the nonresonant $gg \rightarrow 4l$ background. Obtaining this refinement is now possible, because, in [19, 20], the individual contributions to the background are reported separately. Denoting by $\sigma_{\text{B}}^{\text{gg}}$ the pure nonresonant $gg \rightarrow 4l$

Bin [GeV]	$\hat{\sigma}_{\text{EXP}}$ [fb]	$\sigma_{\text{B}}^{\text{gg}}$ [fb]	$(\hat{\sigma}_{\text{EXP}} - \sigma_{\text{B}}^{\text{gg}})$ [fb]
555–585	0.003 ± 0.060	0.023 ± 0.004	-0.020 ± 0.060
585–620	0.105 ± 0.073	0.020 ± 0.003	$+0.085 \pm 0.075$
620–665	0.121 ± 0.078	0.019 ± 0.003	$+0.102 \pm 0.078$
665–720	0.152 ± 0.075	0.016 ± 0.003	$+0.136 \pm 0.075$
720–800	-0.067 ± 0.050	0.013 ± 0.002	-0.080 ± 0.050
800–900	0.062 ± 0.055	0.009 ± 0.002	$+0.053 \pm 0.055$

TABLE 3: For each energy bin, we give the ATLAS experimental cross section $\hat{\sigma}_{\text{EXP}}$ (cf. equation (5)). The two cross sections σ_{EXP} and σ_{B} are listed in Table 2. The other background cross section $\sigma_{\text{B}}^{\text{gg}}$ takes only into account the nonresonant $gg \rightarrow 4l$ process and is computed by multiplying the bin size with the average differential cross section $(d\sigma_{\text{B}}^{\text{gg}}/dE)$ in each bin; see [20].

Bin [GeV]	$\hat{\sigma}_{\text{EXP}}$ [fb]	σ_T [fb]	χ^2
555–585	0.003 ± 0.060	0.048	0.56
585–620	0.105 ± 0.073	0.056	0.45
620–665	0.121 ± 0.078	0.123	0.00
665–720	0.152 ± 0.075	0.152	0.00
720–800	-0.067 ± 0.050	0.002	1.90
800–900	0.062 ± 0.055	0.004	1.11

TABLE 4: Comparing the experimental cross section in Table 3 with the theoretical equation (3) for the optimal set of parameters $M_H = 677$ GeV, $\Gamma_H = 21$ GeV, and $\sigma_R = 0.40$ fb.

background cross section, we can thus consider a corresponding experimental cross section $\hat{\sigma}_{\text{EXP}}$ after subtracting out preliminarily the “non-ggF” background:

$$\hat{\sigma}_{\text{EXP}} = \sigma_{\text{EXP}} - (\sigma_{\text{B}} - \sigma_{\text{B}}^{\text{gg}}). \quad (5)$$

The corresponding values and background are given in Table 3.

We then compare the resulting experimental $\hat{\sigma}_{\text{EXP}}$ with the theoretical σ_T in equation (3), after the identification $\sigma_b = \sigma_{\text{B}}^{\text{gg}}$. By parametrizing the ATLAS differential background $(d\sigma_{\text{B}}^{\text{gg}}/dE) \sim A \times (710 \text{ GeV}/E)^\nu$, with $A \sim (2.42 \pm 0.18) \times 10^{-4}$ fb/GeV and $\nu \sim 5.24 \pm 0.45$, and integrating the various contributions to equation (3) within each energy bin, a fit to the data gives $M_H = 677_{-14}^{+30}$ GeV, $\Gamma_H = 21_{-16}^{+28}$ GeV, and $\sigma_R = 0.40_{-0.34}^{+0.62}$ fb. The comparison of the optimal parameters is shown in Table 4.

The quality of our fit is good, but the error bars are large. Yet, by restricting again to the central values, there is good agreement with our expectations. Indeed, by rescaling the partial width from $\Gamma(H \rightarrow ZZ) \sim 1.6$ GeV to 1.55 GeV (for M_H from 700 to 677 GeV), and fixing $\langle \Gamma_H \rangle = 21$ GeV, we find a branching ratio $B(H \rightarrow ZZ) \sim 0.073$. For the theoretical value $\sigma^{\text{ggF}}(pp \rightarrow H) \sim 1100$ fb of [15] (at $M_H = 677$ GeV), this would then imply a theoretical peak cross section $(\sigma_R)^{\text{Theor}} = 1100 \times 0.073 \times 0.0045 \sim 0.36$ fb, which only differs by 10% from the central value $\langle \sigma_R \rangle = 0.40$ fb of our fit. Moreover, from the central values of the fit $\langle \sigma_R \rangle = 0.40$ fb and $\langle \gamma_H \rangle = 0.031$, we find $\langle \sigma_R \rangle \times \langle \gamma_H \rangle \sim 0.012$ fb, again in good agreement with our equation (2).

Summarizing from the two ATLAS papers [17] and [19], we find consistent indications of a new resonance in our theoretical mass range $(M_H)^{\text{Theor}} \sim 690$ (30) GeV. By comparing with [19], we identify more precisely the nonresonant back-

ground $gg \rightarrow 4l$, which can interfere with a second resonance H produced via gluon-gluon fusion. Thus, the determinations obtained from our equation (3) are more accurate, from a theoretical point of view. In practice, there is not too much difference with the previous [12, 13] based on the ggF -low events of [17]. Indeed, the two mass values $(M_H)^{\text{EXP}} = 677_{-14}^{+30}$ GeV vs. $(M_H)^{\text{EXP}} = 706(25)$ GeV and the two decay widths $\Gamma_H = 21_{-16}^{+28}$ GeV vs. $\Gamma_H = 29 \pm 20$ GeV are well consistent within their uncertainties. Most notably, our crucial correlation equation (2) is well reproduced by the central values of the fits to the two sets of data.

2.2. The ATLAS High-Mass $\gamma\gamma$ Events

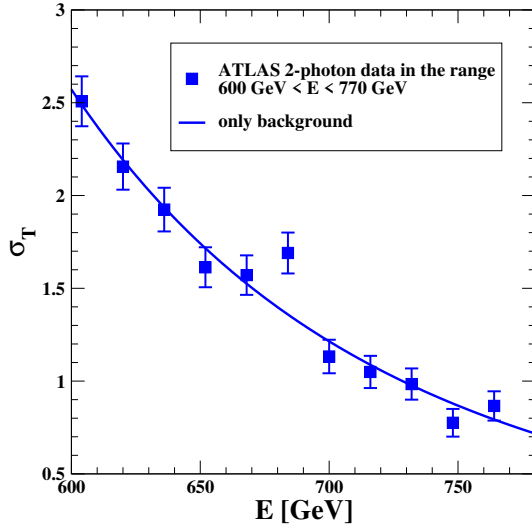


FIGURE 3: The fit with equation (3) and $\sigma_R = 0$ to the ATLAS data [21] shown in Table 5, transformed into cross sections in fb. The χ^2 value is 14, with the background parameters $A = 1.35$ fb and $\nu = 4.87$.

Fit with interference of a background + resonance

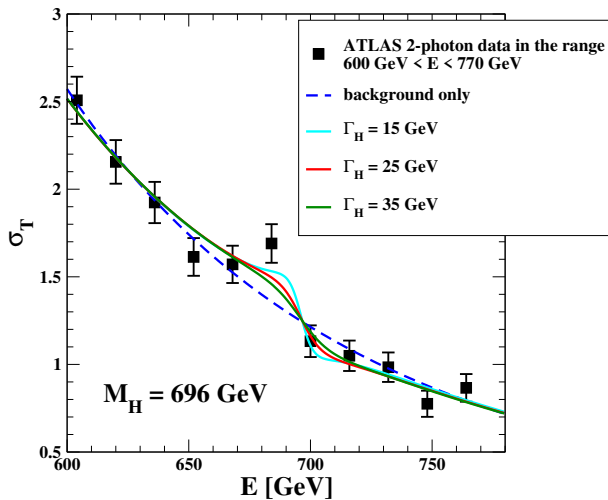


FIGURE 4: Three fits with equation (3) to the ATLAS data [21] in Table 5, transformed into cross sections in fb. The χ^2 values are 7.5, 8.8, and 10.2, for $\Gamma_H = 15, 25$, and 35 GeV, respectively.

μ	604	620	636	652	668	684	700	716	732	748	764
N	349	300	267	224	218	235	157	146	137	108	120

TABLE 5: The ATLAS number $N = N(\gamma\gamma)$ of events, in bins of 16 GeV and for luminosity 139 fb^{-1} , for the range of invariant mass $\mu = \mu(\gamma\gamma) = 600 \div 770$ GeV. These values were extracted from Figure 3 of [21] because the relevant numbers are not reported in the companion HEPData file.

References [12, 13] also considered the invariant-mass distribution of the inclusive diphoton events observed by ATLAS[21]; see Table 5. By parametrizing the background with a power-law form $\sigma_B(E) \sim A \times (685 \text{ GeV}/E)^\nu$, a fit to the data in Table 5 gives a good description of all data points, except for a sizable excess at 684 GeV (estimated by ATLAS to have a local significance of more than 3σ); see Figure 3.

This isolated discrepancy shows how a (hypothetical) new resonance might remain hidden behind a large background nearly everywhere. For this reason, apart from the mass $M_H = 696(12)$ GeV, the total decay width is determined very poorly, namely, $\Gamma_H = 15_{-13}^{+18}$ GeV, but still consistent with the other loose determinations from the 4-lepton data. In Figure 4, we show three fits with the full equation (3), for $\Gamma_H = 15, 25$, and 35 GeV.

2.3. ATLAS and CMS ($b\bar{b} + \gamma\gamma$) Events

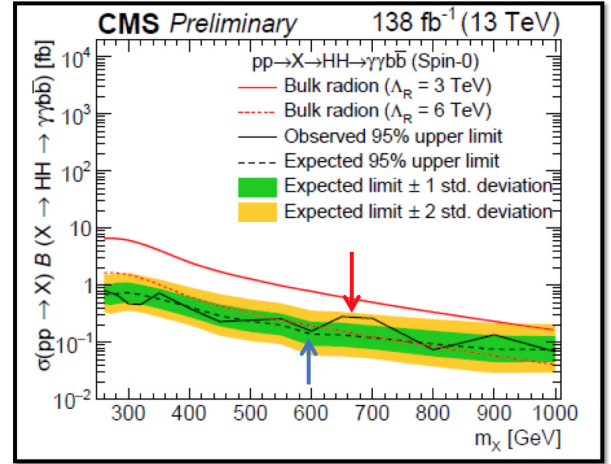


FIGURE 5: Expected and observed 95% upper limit for the cross section $\sigma(pp \rightarrow X \rightarrow h(125)h(125) \rightarrow b\bar{b} + \gamma\gamma)$ observed by the CMS Collaboration [22].

The ATLAS and CMS Collaborations have also searched for new resonances decaying, through two intermediate $h(125)$ scalars, into a $b\bar{b}$ quark pair and a $\gamma\gamma$ pair. In particular, in [22], one considered the cross section for the full process:

$$\sigma(\text{full}) = \sigma(pp \rightarrow X \rightarrow hh \rightarrow b\bar{b} + \gamma\gamma). \quad (6)$$

For a spin-zero resonance, the 95% upper limit $\sigma(\text{full}) < 0.16$ fb, for an invariant mass of 600 GeV, was found to increase by about a factor two, up to $\sigma(\text{full}) < 0.30$ fb in a plateau $650 \div 700$ GeV, and then to decrease for larger energies; see Figure 5.

The local statistical significance is modest, about 1.6σ , but the relevant mass region $M_X \sim 675(25)$ GeV is precise and

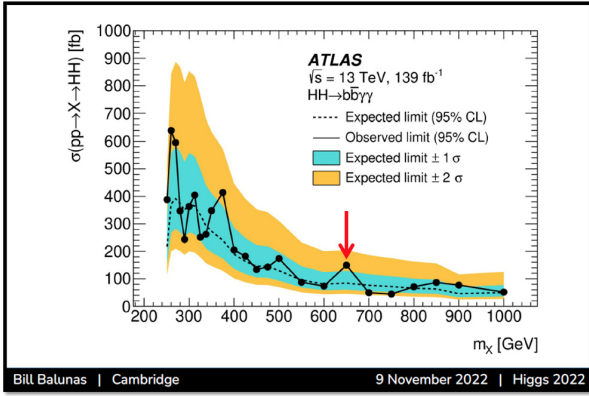


FIGURE 6: Expected and observed 95% upper limit for the cross section $\sigma(pp \rightarrow X \rightarrow h(125)h(125))$ extracted by the ATLAS Collaboration from the final state $(b\bar{b} + \gamma\gamma)$. The figure is taken from the talk given by Bill Balunas at Higgs-2022 and is the same as Figure 15 of the ATLAS paper [23].

agrees well with our prediction. The analogous ATLAS plot is depicted in Figure 6 (which is the same as Figure 15 of the ATLAS paper [23]). Again, one finds a modest 1.2σ excess at 650 (25) GeV immediately followed by a 1.4σ defect, which could indicate a negative above-peak ($M_H^2 - s$) interference effect as found in the ATLAS 4-lepton data.

2.4. CMS-TOTEM $\gamma\gamma$ Events Produced in pp Diffractive Scattering

The CMS and TOTEM Collaborations have also been searching for high-mass photon pairs produced in pp diffractive scattering, i.e., when both final protons are tagged and have large x_F . For our scope, the relevant information is contained in Figure 7, taken from [24]. In the range of invariant mass 650 (40) GeV and for a statistics of 102.7 fb^{-1} , the observed number of $\gamma\gamma$ events is $N^{\text{EXP}} \sim 76$ (9), to be compared with an estimated background $N_B \sim 40$ (9). In the most conservative case, namely, $N_B = 49$, this is a local 3σ effect and is the only statistically significant excess in the plot.

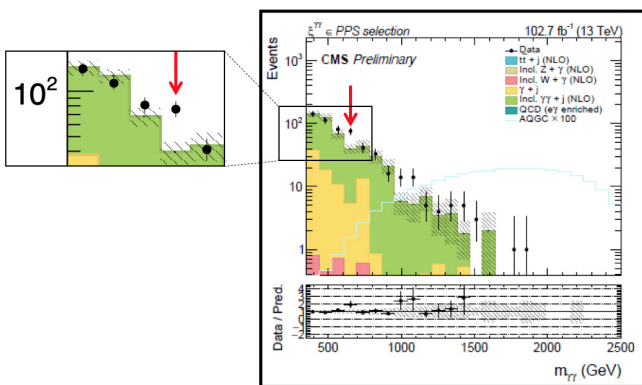


FIGURE 7: The $\gamma\gamma$ events produced in pp diffractive scattering [24]. In the bin 650 (40) GeV, one finds $N^{\text{EXP}} \sim 76$ (9), compared to an estimated background $N_B \sim 40$ (9).

3. SUMMARY AND CONCLUSIONS

Let us summarize our review of LHC data:

- (i) The ATLAS ggF-like four-lepton events [17] reported in Table 1 show a definite excess-defect sequence, suggesting the existence of a new resonance. The same pattern is also visible in the ATLAS cross section [19]; see Table 2 and the $\Delta\sigma$ in Figure 2. The combined statistical deviation in the latter analysis is at the 3σ level and indicates a resonance mass $M_H = 677^{+30}_{-14}$ GeV.
- (ii) Observing the $+3\sigma$ excess at 684 (16) GeV in the inclusive ATLAS $\gamma\gamma$ events [21], a fit to these data was performed in [12, 13]. The resulting mass is $M_H = 696$ (12) GeV.
- (iii) An overall $+2\sigma$ effect in the $(b\bar{b} + \gamma\gamma)$ channel is obtained by combining the excess of events observed by ATLAS at 650 (25) GeV and the corresponding excess observed by CMS at 675 (25) GeV.
- (iv) A $+3\sigma$ excess is present at 650 (40) GeV in the distribution of CMS-TOTEM $\gamma\gamma$ events produced in pp diffractive scattering.

By combining the above determinations (i)–(iv), the resulting estimate $(M_H)^{\text{EXP}} \sim 682$ (10) GeV is in very good agreement with our expectation $(M_H)^{\text{Theor}} = 690$ (30) GeV. We stress again that, when comparing with a definite prediction, one should look for deviations from the background nearby, so that local significance is not downgraded by the so-called “look elsewhere” effect. Therefore, since the correlation of the above measurements is small, the combined statistical evidence for a new resonance in the expected mass range is far from negligible and close to (if not above) the traditional 5σ level. We also emphasize that the determinations (i) and (ii) above were obtained by fitting the numerical data reported in [17, 19, 21] to the general expressions equations (3) and (4). This is very different from comparing with other Beyond-Standard-Model scenarios (such as supersymmetry and extra-dimensions), whose exclusion limits assume built-in constraints (such as mass-width and/or mass-couplings relations) that are not valid in our approach. For this reason, we look forward to new precise data on which we can carry out the same general analysis as with the ATLAS papers [17, 19, 21].

CONFLICTS OF INTEREST

The authors declare that there are no conflicts of interest regarding the publication of this paper.

References

- [1] G. Aad et al. [ATLAS Collaboration], Phys. Lett. B **716**, 1 (2012).
- [2] S. Chatrchyan et al. [CMS Collaboration], Phys. Lett. B **716**, 30 (2012).
- [3] V. Branchina, E. Messina, Phys. Rev. Lett. **111**, 241801 (2013).
- [4] E. Gabrielli, et al., Phys. Rev. D **89**, 015017 (2014).
- [5] G. Degrossi et al., JHEP **08**, 098 (2012).
- [6] M. Consoli and L. Cosmai, Int.J.Mod.Phys. A **35**, 2050103(2020).

- [7] M. Consoli and L. Cosmai, “Spontaneous Symmetry Breaking and Its Pattern of Scales,” *Symmetry* **12**, 2037 (2020).
- [8] M. Consoli, “A Hidden, Heavier Resonance of the Higgs Field,” Contribution to Veltman Memorial Volume, *Acta Phys. Polon. B* **52**, 763 (2021).
- [9] M. Consoli and G. Rupp, “Second resonance of the Higgs field: motivations, experimental signals, unitarity constraints,” arXiv:2308.01429 [hep-ph].
- [10] M. Consoli and L. Cosmai, *Int.J.Mod.Phys.A* **37**, 2250091 (2022).
- [11] M. Consoli, L. Cosmai, and F. Fabbri, “Experimental signals for a new heavy resonance in the ATLAS and CMS data,” in Proceedings of ICHEP 2022, PoS **ICHEP2022**, 204 (2022).
- [12] M. Consoli, L. Cosmai, and F. Fabbri, arXiv:2208.00920 [hep-ph].
- [13] M. Consoli, L. Cosmai, and F. Fabbri, MDPI Special Issue, “BSM and Higgs Physics,” *Universe* **9**, 99 (2023).
- [14] <https://twiki.cern.ch/twiki/bin/view/LHCPhysics/CERNYellowReportPageBSMA13TeV>.
- [15] <https://twiki.cern.ch/twiki/bin/view/LHCPhysics/CERNYellowReportPageAt13TeV>.
- [16] A. M. Sirunyan et al. [CMS Collaboration], “Measurements of $t\bar{t}$ differential cross sections in proton-proton collisions at $\sqrt{s} = 13$ TeV using events containing two leptons,” *JHEP* **02**, 149 (2019).
- [17] G. Aad et al. [ATLAS Collaboration], “Search for heavy resonances decaying into a pair of Z bosons in the $\ell^+\ell^-\ell'^+\ell'^-$ and $\ell^+\ell^-\nu\bar{\nu}$ final states using 139 fb⁻¹ of proton-proton collisions at $\sqrt{s} = 13$ TeV with the ATLAS detector,” *Eur. Phys. J. C* **81**, 332 (2021).
- [18] ATLAS Collaboration, <https://www.hepdata.net/record/ins1820316>.
- [19] G. Aad et al. [ATLAS Collaboration], “Measurements of differential cross-sections in four-lepton events in 13 TeV proton-proton collisions with the ATLAS detector,” *JHEP* **07**, 005 (2021).
- [20] ATLAS Collaboration, <https://www.hepdata.net/record/ins1849535>.
- [21] G. Aad et al. [ATLAS Collaboration], “Search for resonances decaying into photon pairs in 139 fb⁻¹ of pp collisions at $\sqrt{s} = 13$ TeV with the ATLAS detector,” *Phys. Lett. B* **822**, 136651 (2021).
- [22] CMS Collaboration, “Search for a new resonance decaying to two scalars in the final state with two bottom quarks and two photons in proton-proton collisions at $\sqrt{s} = 13$ TeV,” arXiv:2310.01643 [hep-ex].
- [23] G. Aad et al. [ATLAS Collaboration], “Search for Higgs boson pair production in the two bottom quarks plus two photons final state in pp collisions at $\sqrt{s} = 13$ TeV with the ATLAS detector,” *Phys. Rev. D* **106**, 052001 (2022).
- [24] CMS and TOTEM Collaborations, arXiv:2311.02725 [hep-ex].